

Persistent Current of $SU(N)$ Fermions

Wayne J. Chetcuti,^{1,2} Tobias Haug,³ Leong-Chuan Kwek,^{3,4} and Luigi Amico^{3,5,6,7,*}

¹Dipartimento di Fisica e Astronomia, Via S. Sofia 64, 95127 Catania, Italy

²INFN-Sezione di Catania, Via S. Sofia 64, 95127 Catania, Italy

³Centre for Quantum Technologies, National University of Singapore, 3 Science Drive 2, Singapore 117543, Singapore

⁴MajuLab, CNRS-UNS-NUS-NTU International Joint Research Unit, UMI 3654, Singapore

⁵Quantum Research Centre, Technology Innovation Institute, Abu Dhabi, UAE

⁶CNR-MATIS-IMM & INFN-Sezione di Catania, Via S. Sofia 64, 95127 Catania, Italy

⁷LANEF 'Chaire d'excellence', Université Grenoble-Alpes & CNRS, F-38000 Grenoble, France

(Dated: January 27, 2022)

We study the persistent current in a system of $SU(N)$ fermions with repulsive interaction confined in a ring-shaped potential and pierced by an effective magnetic flux. By applying a combination of Bethe ansatz and numerical analysis, we demonstrate that, as a combined effect of spin correlations, interactions and applied flux a specific phenomenon can occur in the system: spinon creation in the ground state. As a consequence, peculiar features in the persistent current arise. The elementary flux quantum, which fixes the persistent current periodicity, is observed to evolve from a single particle one to an extreme case of fractional flux quantum, in which one quantum is shared by all the particles. We show that the persistent current depends on the number of spin components N , number of particles and interaction in a specific way that in certain physical regimes has universality traits. At integer filling fractions, the persistent current is suppressed above a threshold of the repulsive interaction by the Mott spectral gap. Despite its mesoscopic nature, the current displays a clear finite size scaling behavior. Specific parity effects in the persistent current landscape hold.

Introduction – Quantum technology intertwines basic research in quantum physics and technology to an unprecedented degree: different quantum systems, manipulated and controlled from the macroscopic spatial scale down to individual or atomic level, can be platforms for quantum devices and simulators with refined capabilities; on the other hand, the acquired technology prompts new studies of fundamental aspects of quantum science with an enhanced precision and sensitivity. Amongst the various quantum systems relevant for quantum technologies, ultracold atomic systems play an important role due to their excellent coherent properties and enhanced control and flexibility of the operating conditions [1]. Atomtronics is an emerging research area in quantum technology exploiting cold atoms matter-wave circuits with a variety of different architectures [2].

Being characterized by distinctive physical principles, atomic circuits can define a quantum technology with specific features. In particular, one of the peculiar knobs that can be exploited in atomtronics is the statistics of the particles forming the quantum fluid flowing in the circuit. Most of the studies carried out so far have been devoted to atomtronic circuits of ultracold bosons, whilst ones comprised of interacting ultracold fermions require extensive investigations.

In this paper, we focus on quantum fluids comprising of interacting multicomponent spin $SU(N)$ fermions. Strongly interacting fermions with N spin components, as provided by alkaline-earth and ytterbium cold atomic gas, are highly non-trivial multicomponent quantum systems. Such systems extend beyond the physics of interacting spin- $\frac{1}{2}$ electrons found in condensed matter systems [3, 4]. They are very relevant both for high-precision measurement [5–7] and to enlarge the scope of cold atoms quantum simulators of many-body systems [8, 9]. Additionally, atom-atom interactions can be made independent on the nuclear spin. This feature effectively en-

larges the symmetry of the systems to the $SU(N)$ one. Such a feature makes cold alkaline-earth atoms, especially with lattice confinements, an ideal platform to study exotic quantum matter, including higher spin magnetism, spin liquids and topological matter [10–12] and, beyond condensed matter physics, in QCD [13].

Here, we consider N_p fermions with $SU(N)$ symmetry trapped in a ring-shaped circuit of mesoscopic size L and pierced by an effective magnetic field. We will study the persistent current response to this applied field.

We will explore different regimes depending on the filling fraction N_p/L . *i)* For incommensurate N_p/L , the persistent current is non-vanishing for any value of interaction. Monitoring the numerical results for the spectrum of the system with the exact Bethe ansatz solution [14], we find that *as the effective magnetic flux increases, spinon excitations can be created in the ground state*. Such a remarkable phenomenon occurs as a specific ‘screening’ of the external flux, which being a quantity that can be adjusted continuously, can be compensated by spinons excitations (that are quantized in nature) only partially. This in turn results in an imbalance and causes the persistent current to display characteristic oscillations with a period of $1/N_p$ shorter than the bare flux quantum. For two-spin-component fermions in the large interaction regime, such a phenomenon was studied in [15, 16]. We shall see that such a process depends on N_p , number of spin components and interaction in a non-trivial way. *ii)* In contrast with the $SU(2)$ case [17], $SU(N)$ fermions with $N > 2$ at integer fillings undergo a Mott quantum phase transition for a finite value of interaction $U = U_c$. Accordingly, we find that a metallic behaviour crossovers to a regime in which the current is exponentially suppressed. This regime is also monitored by Bethe ansatz [18] and corroborated by exact diagonalization and DMRG [19]. We shall see that, *despite the persistent cur-*

rent being mesoscopic in nature, the onset of the Mott transition is marked by a clear finite size scaling. We shall see that the onset to the gapped phase progressively hinders the spinon creation phenomenon. *iii)* For both non-integer and integer fillings fractions, we demonstrate how results of Byers-Yang, Onsager and Leggett on the landscape of the system persistent current can be generalized to $SU(N)$ fermions [20–22].

Methods – A system of N_p $SU(N)$ fermions residing in a ring-shaped lattice composed of L sites threaded with a magnetic flux ϕ can be modeled using the Hubbard model [10]

$$\mathcal{H}_{SU(N)} = -t \sum_{j=1}^L \sum_{\alpha=1}^N (e^{i\frac{2\pi\phi}{L}} c_{\alpha,j}^\dagger c_{\alpha,j+1} + \text{h.c.}) + \frac{U}{2} \sum_j n_j(n_j - 1) \quad (1)$$

where $c_{\alpha,j}^\dagger$ ($c_{\alpha,j}$) creates (annihilates) a fermion with colour α , $n_j = \sum_\alpha c_{\alpha,j}^\dagger c_{\alpha,j}$ is the local particle number operator for site j . The parameters t and U account for the hopping strength and on-site interaction respectively, with the latter being required to be greater than zero in order to have repulsive interactions. The effective magnetic field is realized through the Peierls substitution $t \rightarrow te^{i\frac{2\pi\phi}{L}}$. For $N = 2$, the Hubbard model describing spin- $\frac{1}{2}$ fermions is obtained. In this case, the Hamiltonian (1) is integrable by Bethe ansatz for any values of the system parameters and filling fractions $\nu = N_p/L$ [17]. For $N > 2$, the Bethe ansatz integrability is preserved in the continuous limit of vanishing lattice spacing, (1) turning into the Gaudin-Yang-Sutherland model describing $SU(N)$ fermions with delta interaction [14] (see also [23]); such a regime is achieved by (1) in the dilute limit of small fillings fractions ν . Another integrable regime of (1) is obtained for $n_j = 1\forall j$ and large repulsive values of $U \gg t$ for which the system is governed by the Lai-Sutherland model [10, 18]. The Bethe ansatz eigenstates are customarily labeled by a certain set of quantum numbers $\{I_a, J_\beta\}$, $a = 1 \dots N_p$ and $\beta, j = 1 \dots N - 1$. At zero flux ϕ , the ground state is characterized by consecutive quantum numbers $\{I_a, J_\beta\}$. Instead, configurations of quantum numbers with ‘holes’ correspond to excitations; in particular holes in $\{J_\beta\}$ characterize the so called spinon excitations [24]. For $SU(N)$ fermions, there can be $N - 1$ different types of such spinon states [25, 26]. For non-vanishing ϕ , we shall see the quantum numbers configurations $\{I_a, J_\beta\}$ can change. In the intermediate interactions and intermediate fillings, the model (1) is not integrable and approximated methods are needed to access its spectrum. Indeed, Hubbard models for $SU(2)$ and $SU(N)$ fermions enjoy very different physics implying. For incommensurate fillings, a metallic behaviour is found with characteristic oscillations of the spin-spin and charge correlation functions that, for $N > 2$ can be coupled each other. At integer filling fractions, two component fermions are in a Mott phase. Notably, such phase is suppressed only exponentially for $N = 2$ [17]; in striking contrast, for $N > 2$ the system displays a Mott transition for a finite value of U/t [10] (see also [27]).

At mesoscopic size, the properties discussed above are displayed as specific phenomena. In this regime, even though the

application of the magnetic flux does not change the nature of the possible excitations, we shall see that the latter may be indeed promoted to ground states. Our diagnostic tool is the persistent current. At zero temperature the persistent current of the system is given by

$$I(\phi) = -\frac{\partial E_0}{\partial \phi} \quad (2)$$

where E_0 is the groundstate energy. For a quantum system in a ring the angular momentum is quantized (see [28, 29] for recent experiments). Accordingly, $I(\phi)$ displays a characteristic sawtooth behaviour, with a periodicity that Leggett proved to be fixed by the effective flux quantum ϕ_0 of the system [20–22]. Furthermore, the persistent current is parity dependent: for systems with even (odd) number of spinless particles, the energy is decreased (increased) by the application of the external flux; therefore, the persistent current displays a paramagnetic (diamagnetic) behaviour. Leggett predictions are independent of disorder. We shall see how specific parity effects holds for $SU(N)$ systems.

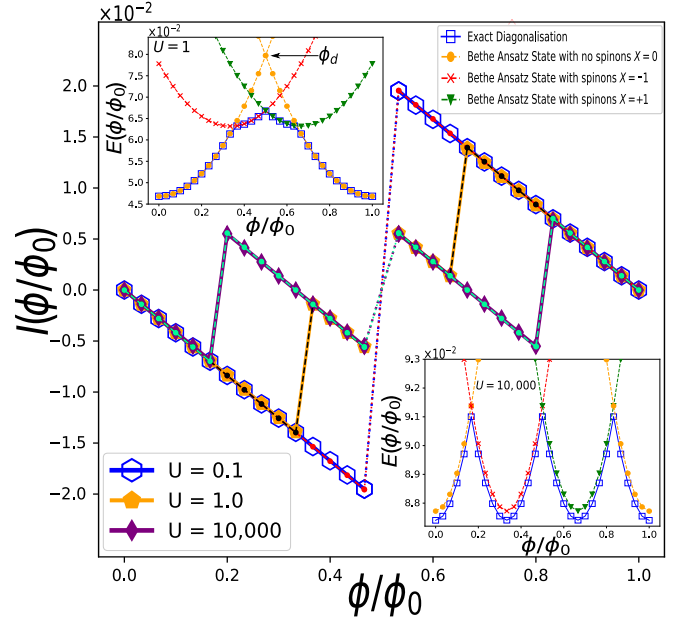


FIG. 1. Persistent current $I(\phi)$ at incommensurate filling for $SU(3)$ fermions with different interaction strengths U in the dilute filling regime of the Hubbard model. The exact diagonalization $L = 30, N_p = 3$ is monitored with the Bethe ansatz of the Sutherland-Gaudin-Yang model. The Insets show how the Bethe ansatz energies need to be characterized by spinon quantum numbers in order to be the actual ground state. At $U = 0$, the ground state energy is a periodic sequence of parabolas meeting at degeneracy points ϕ_d ($\phi_d = 1/2$ for the case displayed in the figure).

In our approach, we combine exact diagonalization or DMRG analysis with, whenever possible, Bethe ansatz results. Specifically: in the integrable regimes of dilute systems (described by Gaudin-Yang-Sutherland model) and half-filling & large interactions (captured by the Sutherland

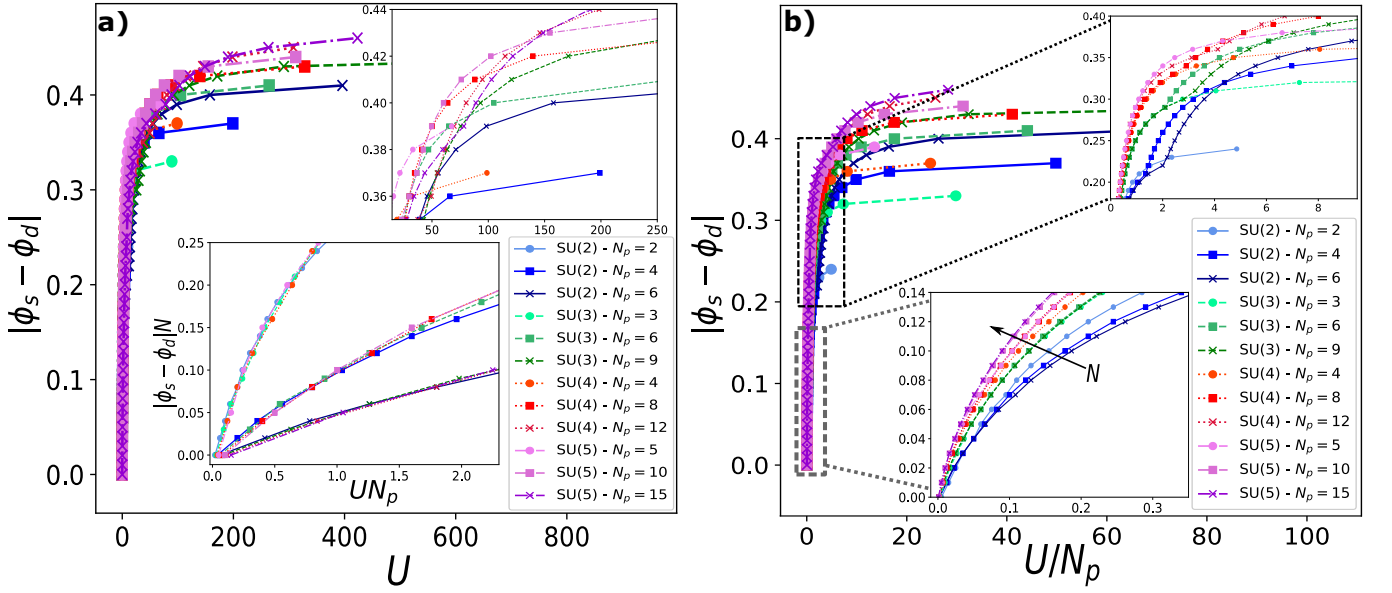


FIG. 2. Figures of merit for spinon creation in the ground state of $SU(N)$ fermions. We consider the minimum value of U required for spinons to be created in the groundstate for a given value of ϕ ; all the values of ϕ where a spinon is created are recorded. The displayed curves are calculated by monitoring all the distances $|\phi_s - \phi_d|$ at which the state with no spinons crosses states with any spinon configurations where ϕ_s is the flux at which spinons are created and ϕ_d is the degeneracy point (see Fig. 1). **a)** Spinon creation flux distance $|\phi_s - \phi_d|$ against interaction U . The top inset contains the data in the intermediate U regime. The bottom inset depicts the spinon creation flux distance against the interaction, rescaled by N and N_p respectively, in the limit of low U/N_p . **b)** Spinon creation flux distance $|\phi_s - \phi_d|$ against interaction per particle U/N_p . The bottom inset (grey) contains data in the low U/N_p regime, whilst the top inset (black) is the data in the intermediate U/N_p regime. The discontinuities observed in the intermediate U/N_p regime when $N_p/N > 1$, are more pronounced for larger values of N_p/N for a system with the same N_p but different N . All the presented results are obtained by Bethe ansatz of Gaudin-Yang-Sutherland model for $L = 40$, with $N_p = 1$ (circles), 2(squares), 3(crosses) per spin component, with $N = 2, 3, 4, 5$. Thus the dilute limit of the Hubbard model (1) is covered.

model), the Bethe ansatz results (through the Bethe quantum numbers introduced above) are exploited as bookkeeping to monitor the eigenstates provided by the numerical results. This way, we can establish the nature and the physical content of the ground state of the system as functions of the parameters. In particular, the actual lowest energy of the system can be obtained only by assuming specific configurations of the Bethe quantum numbers corresponding to spinon excitations. In the non-integrable regimes, we rely on the numerical analysis. In this article, only systems with singlet states for which the total magnetization $S^z = 0$ are considered. In the following, the energy scale is given by $t = 1$.

Persistent current of $SU(N)$ fermions at incommensurate fillings— We start our analysis in the low filling regimes (continuous limit) in which we can rely on exact results based on the Gaudin-Yang-Sutherland model Bethe ansatz. The numerical analysis shows that, by increasing ϕ , specific energy level crossings occur in the ground state of the system. The Bethe ansatz analysis (see Supplemental material) allow to recognize such level crossings as ground state transitions between no-spinons states (characterized by consecutive $\{J_\beta\}$) and spinons states (characterized by the presence of holes in the $\{J_\beta\}$ configurations). Specific $1/N_p$ periodic oscillations occur in the ground state energy as ϕ is varied; therefore, a curve with N_p cusps/parabolic-wise segments per flux quantum is produced. Such feature was evidenced for two spin

component fermions in the large interaction regime [15, 16]. Here, we find that the spinon creation defines a phenomenon occurring for any value of U ; in addition, we shall see that the spinon creation mechanism displays a non-trivial dependence on the number of spin components N . Indeed, the different $N - 1$ spinon configurations are found to play a relevant role for the phenomenon. The quantity $X = \sum_j^{N-1} \sum_{\beta_j} J_{\beta_j}$ can be exploited to characterize the properties of the specific spinon excitation that is created in the ground state.

Specifically, for small and intermediate U , while the system's ground state with no spinons is found to be non-degenerate, the ground state with spinons can be made of degenerate multiplets corresponding to Bethe states with distinct configurations of the quantum numbers J_{β_j} (see the inset of Fig. 1). By further increasing U , the spinons states organize themselves in multiplets of increasing degeneracy on a wider interval of the flux.

At large but finite U , the exact Bethe ansatz analysis shows that the spectrum can be reproduced by a suitable continuous limit of a $SU(N)$ $t - J_{eff}$ model with $J_{eff} = 4E_\infty/(UL)$, where E_∞ is the energy of the Gaudin-Yang-Sutherland model at infinite interaction (see Supplementary material). We remark that the specific features of the $SU(N)$ fermions enter the entire energy spectrum of the system through the $SU(N)$ quantum numbers $\{I_a, J_{\beta_j}\}$. In the limit of infinite U , the persistent current is analytically obtained as (see the Supplementary ma-

terial for derivations)

$$I(\phi) = -2 \left(\frac{2\pi}{L} \right)^2 \sum_a^{N_p} \left[I_a + \frac{X}{N_p} + \phi \right] \quad (3)$$

The above expression shows that, in this regime, the persistent current displays $1/N_p$ reduced periodicity; such a phenomenon is observed for $UL/N_p \gg 1$, for any number of spin components N . Therefore, in this regime, *the bare flux quantum of the system results to be evenly shared among all the particles*. We note that, in the infinite U regime, the ground state reaches the highest degeneracy (see inset of Fig. 1).

As a global view of the spinon creation in the ground state phenomenon, we monitor, for different values of U , N , and N_p , the values of the flux ϕ_s at which the ground state energy in the system is no longer given by a state with no spinons – Fig. 2. *At moderate U spinon production is found to be a universal function of the N_p/N – see the lower inset of Fig. 2a; for systems with lower N_p , spinon creation is generated at a lower value of interaction. For large U , we observe that the spinon production is dictated by N_p , with a fine structure that is determined by N : Systems with higher N_p produce spinons at a lower value of U ; with N_p fixed, systems with the lower value of N_p/N generate spinons at a lower U . Such a phenomenon depends on the specific degeneracies of systems discussed previously that facilitate the creation of spinons by increasing N . This feature emerges also by analysing the dependence of the phenomenon on the interaction per particle U/N_p – Fig. 2b. We observe that N enhances the spinon production – see the lower inset of Fig. 2b. We also note that, while the number of spinons decreases with N_p for two-component fermions, for $N > 2$ such trend appears to be reversed. For intermediate values of U , discontinuities arise in the curves in the cases where $N/N_p > 1$ (Fig. 2b). These discontinuities correspond to jumps ΔX in the spinon character X . By comparing systems with the same N_p but for different N , we note that the discontinuities tend to be smoothed out by increasing N and L (see Supplementary material). We also note that the value of ΔX results to be parity dependent (see below).*

Commensurate fillings regime– At integer filling fractions $\sum_j^L n_j = 1$, the system enters a Mott phase for $U > U_c$ (thermodynamic limit). In this phase, a spectral gap opens. For small U , the current is a nearly perfect sawtooth. For our mesoscopic system, we observe that indeed such behavior of $I(\phi)$ is smoothed out indicating the onset of the Mott phase transition by increasing U (see Fig. 3a). Such a behavior is found to hold for all N . The gap indicating the onset of the Mott phase transition is studied in Fig. 3c (see also Supplementary material). For the case $N = 2$ such gap opens at $U = 0$; for $N > 2$ the spectral gap opens at a finite value of U . Both the current amplitude $I_{\max} = \max_{\phi}(I)$ and ΔE_0 are suppressed exponentially for large U – Fig. 3b and Fig. 3c. The scaling of the suppression depends on the size of the system. ΔE_0 around the same specific value U for larger system sizes ($L \geq 8$), which depends on N ($U \approx 2$ for $N = 3$, $U \approx 3$ for $N = 4$). We carry out a finite size scaling analysis [30] of the

current I for values of interactions around the Mott instability. Fig. 4a the persistent currents display a crossing point at a particular value $U^* \approx 2.9$ (see also [31–34]); a clear data collapse is obtained in Fig. 4b.

The onset to a gapped phase affects the spinon creation process substantially. For two-component fermions ($U^* = 0$), we find that spinon states have energies larger than the ground state energy for any value of U . In contrast, for $N > 2$ spinons can be created for $U < U^*$ following a similar mechanism found for the incommensurate filling cases (see the inset of Fig. 3a); for $U > U^*$ spinon energies result to be well separated by the ground state energy. We note that the Sutherland-Lai Bethe ansatz results can reproduce the qualitative features of the low lying states of the model also for intermediate U obtained by numerics (where the Hubbard model is non integrable); as expected, for large U , Bethe ansatz and numerics match exactly (see Supplementary material).

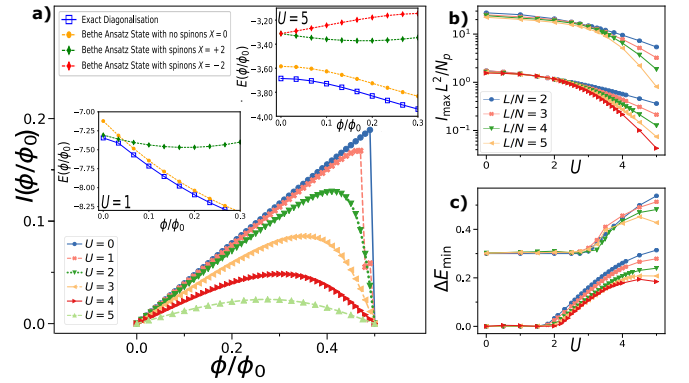


FIG. 3. $SU(N)$ persistent current at integer filling. **a)** Persistent current $I(\phi)$ for $N = 3$, $L = 9$. **b)** The energy gap is determined as the minimal gap for any flux $\Delta E_0 = \min_{\phi}(\Delta E)$. Insets display the Bethe ansatz results of the Sutherland-Lai model compared with the results obtained with exact diagonalizations. The ground state energy at small ϕ can be reached only with spinon configuration of the Bethe quantum number. **b)** Maximal current $I_{\max} = \max_{\phi}(I)$ for $N = 3$ (lower curves) and $N = 4$ (upper curves, shifted by factor 20) plotted against interaction U . **c)** Minimal energy gap E_{\min} against U for $N = 3$ (lower curves) and $N = 4$ (upper curves, shifted by 0.3). All curves with $L > 9$ are calculated with DMRG.

Parity effects– Specific parity effects are observed for $SU(N)$ fermions. Both for commensurate and incommensurate fillings, the persistent current is found diamagnetic (paramagnetic) for ring systems containing $N_p = (2n + 1)N$ ($N_p = (2n)N$) fermions, with n being an integer. The nature of the current can be deduced by looking at the ground state energy of the system, whereby if the system has a minimum (maximum) at zero flux, then it is diamagnetic (paramagnetic) – Fig. 5. Such a parity effect holds for small and intermediate U but it is washed out at infinite U for incommensurate fillings or above a finite threshold of interaction for integer fillings. Indeed, the character of the current is diamagnetic, since the fractionalization of the bare flux quantum causes the ground state energy to always be a minimum at zero flux. Such phenomena generalize the $4n/4n + 2$ of spin- $\frac{1}{2}$ fermions [35].

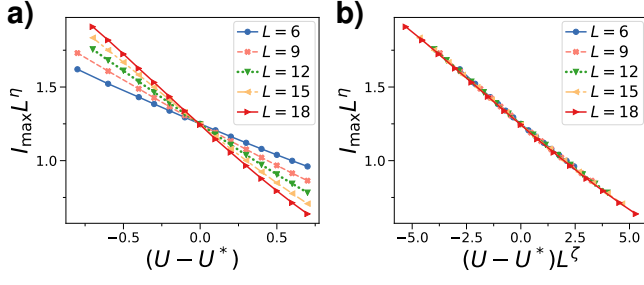


FIG. 4. Finite size scaling of the persistent current. The case $N = 3$ is considered. **a)** Finite size critical crossing of I_{\max} at $U^* = 2.9$ **b)** Data collapse. $L = 6, 9$ were calculated with exact diagonalization; larger L were obtained with DMRG. The critical indices are $\eta \approx 0.2$ and $\zeta \approx 0.7$

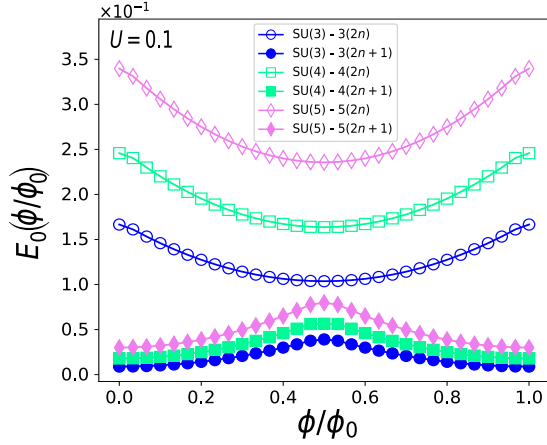


FIG. 5. Parity effect for $SU(N)$ fermions. Ground state energy $E_0(\phi)$ is plotted against the flux ϕ for different N ranging from 3 (circles) to 5 (diamonds). Since the energy is suppressed (increased) by the effective magnetic field, systems with even (odd) number of particle per spin component are paramagnetic (diamagnetic). All the presented results are obtained by Bethe ansatz of Gaudin-Yang-Sutherland model for $L = 30$, with N_p taken to be 1 particle and 2 particles per species for each N corresponding to $n = 0, 1$ respectively.

Conclusions— In this work, we studied the persistent current of a gas of N_p strongly interacting fermions with N spin components. The analysis is carried out for incommensurate and commensurate filling regimes. We highlight the nature of the ground state of the system by corroborating the numerical analysis (exact diagonalization and DMRG) with Bethe ansatz study which allows a reliable access to the specific physical nature of the system's states. Both for incommensurate and commensurate fillings the ground state can have spinon nature. Such a phenomenon implies that the spin correlations can lead to a re-definition of the effective flux quantum of the system and, for incommensurate filling cases, yields the $1/N_p$ fractional periodicity for the persistent current that is observed at large U (see the insets of Fig. 1). This way, the persistent current manifests the specific coupling between the spin and

matter degrees of freedom occurring in $SU(N)$ fermionic systems. The ground state spinon creation displays a marked dependence on the number of spin components with distinctions between the $SU(2)$ and $SU(N)$, $N > 2$ cases (see Fig. 2). In particular, because of the specific $N - 1$ types of excitations, spinon creation is facilitated with increasing N . At moderate U , spinon production is found to be a universal function of N_p/N – see the lower inset of Fig. 2. In the case of integer filling fractions, the creation of spinons is suppressed by increasing U . The sawtooth shape of the current smoothens out to a sinusoidal one (see Fig. 3). This feature arises since the Mott gap prevents level crossings between the groundstate and hinders, besides the motion of the particles, also the creation of spinons in the ground state. Remarkably, a clear finite size scaling behaviour is observed for $N > 2$ even though the persistent current is a mesoscopic quantity (see Fig. 4). A specific parity effect is demonstrated to occur whereby the current is of diamagnetic (paramagnetic) nature for systems comprised of $(2n + 1)N$ ($(2n)N$) number of fermions (see Fig. 5). This parity effect is found to be washed out in the large U regime (see Supplementary material).

We believe that systems in physical conditions and parameter ranges as discussed in the present work can be realized experimentally on several physical platforms, including cold atom quantum technology [3, 4, 36, 37] with the twist provided by atomtronics. In particular, the momentum distribution through the time of flight expansion of cold atom systems has been demonstrated to provide a precise probe for persistent current [2].

Acknowledgements We thank Anna Minguzzi for discussions. The Grenoble LANEF framework ANR-10-LABX-51-01 are acknowledged for their support with mutualized infrastructure.

* On leave from Dipartimento di Fisica e Astronomia 'Ettore Majorana', Università di Catania, Italy

- [1] A. Acín, I. Bloch, H. Buhrman, T. Calarco, C. Eichler, J. Eisert, D. Esteve, N. Gisin, S. J. Glaser, F. Jelezko, S. Kuhr, M. Lewenstein, M. F. Riedel, P. O. Schmidt, R. Thew, A. Wallraff, I. Walmsley, and F. K. Wilhelm, *New Journal of Physics* **20**, 080201 (2018).
- [2] L. Amico, M. Boshier, G. Birkel, A. Minguzzi, C. Miniatura, L. C. Kwek, D. Aghamalyan, V. Ahufinger, N. Andrei, A. S. Arnold, M. Baker, T. A. Bell, T. Bland, J. P. Brantut, D. Cassettari, F. Chevy, R. Citro, S. D. Palo, R. Dumke, M. Edwards, R. Folman, J. Fortagh, S. A. Gardiner, B. M. Garraway, G. Gauthier, A. Günther, T. Haug, C. Hufnagel, M. Keil, W. von Klitzing, P. Ireland, M. Lebrat, W. Li, L. Longchambon, J. Mompart, O. Morsch, P. Naldesi, T. W. Neely, M. Olshanii, E. Orignac, S. Pandey, A. Pérez-Obiol, H. Perrin, L. Piroli, J. Polo, A. L. Pritchard, N. P. Proukakis, C. Rylands, H. Rubinsztein-Dunlop, F. Scazza, S. Stringari, F. Tosto, A. Trombettoni, N. Victorin, D. Wilkowski, K. Xhani, and A. Yakimenko, "Roadmap on atomtronics," (2020), [arXiv:2008.04439 \[cond-mat.quant-gas\]](https://arxiv.org/abs/2008.04439).
- [3] G. Pagano, M. Mancini, G. Cappellini, L. Livi, C. Sias, J. Catani, M. Inguscio, and L. Fallani, *Physical review letters*

- 115**, 265301 (2015).
- [4] G. Cappellini, M. Mancini, G. Pagano, P. Lombardi, L. Livi, M. Siciliani de Cumis, P. Cancio, M. Pizzocaro, D. Calonico, F. Levi, C. Sias, J. Catani, M. Inguscio, and L. Fallani, *Phys. Rev. Lett.* **113**, 120402 (2014).
 - [5] A. D. Ludlow, M. M. Boyd, J. Ye, E. Peik, and P. O. Schmidt, *Rev. Mod. Phys.* **87**, 637 (2015).
 - [6] G. E. Marti, R. B. Hutson, A. Goban, S. L. Campbell, N. Poli, and J. Ye, *Phys. Rev. Lett.* **120**, 103201 (2018).
 - [7] N. Poli, C. Oates, P. Gill, and G. Tino, *La rivista del Nuovo Cimento* **36**, 555 (2013).
 - [8] L. Livi, G. Cappellini, M. Diem, L. Franchi, C. Clivati, M. Frittelli, F. Levi, D. Calonico, J. Catani, M. Inguscio, *et al.*, *Physical review letters* **117**, 220401 (2016).
 - [9] S. Kolkowitz, S. Bromley, T. Bothwell, M. Wall, G. Marti, A. Koller, X. Zhang, A. Rey, and J. Ye, *Nature* **542**, 66 (2017).
 - [10] S. Capponi, P. Lecheminant, and K. Totsuka, *Annals of Physics* **367**, 50 (2016).
 - [11] M. A. Cazalilla and A. M. Rey, *Reports on Progress in Physics* **77**, 124401 (2014).
 - [12] X.-W. Guan, M. T. Batchelor, and C. Lee, *Rev. Mod. Phys.* **85**, 1633 (2013).
 - [13] U.-J. Wiese, *Nuclear Physics A* **931**, 246 (2014).
 - [14] B. Sutherland, *Phys. Rev. Lett.* **20**, 98 (1968).
 - [15] F. V. Kusmartsev, *Journal of Physics: Condensed Matter* **3**, 3199 (1991).
 - [16] N. Yu and M. Fowler, *Phys. Rev. B* **45**, 11795 (1992).
 - [17] E. H. Lieb and F. Y. Wu, *Phys. Rev. Lett.* **20**, 1445 (1968).
 - [18] B. Sutherland, *Phys. Rev. B* **12**, 3795 (1975).
 - [19] E. M. Stoudenmire and S. R. White, *Tensor Library (version 3.1)*.
 - [20] N. Byers and C. Yang, *Physical Review Letters* **7**, 46 (1961).
 - [21] L. Onsager, *Physical Review Letters* **7**, 50 (1961).
 - [22] A. Leggett, in *C.W.J. Beenakker, et al, Granular Nanoelectronics* (Plenum Press, New York, 1991) p. 359.
 - [23] J. Decamp, J. Jünemann, M. Albert, M. Rizzi, A. Minguzzi, and P. Vignolo, *Physical Review A* **94**, 053614 (2016).
 - [24] N. Andrei, *Low-Dimensional Quantum Field Theories for Condensed Matter Physicists* (World Scientific Publishing Co, 2013) pp , 457 (1995).
 - [25] H. Frahm and A. Schadschneider, “On the bethe ansatz soluble degenerate hubbard model,” in *The Hubbard Model: Its Physics and Mathematical Physics*, edited by D. Baeriswyl, D. K. Campbell, J. M. P. Carmelo, F. Guinea, and E. Louis (Springer US, Boston, MA, 1995) pp. 21–28.
 - [26] K.-J.-B. Lee and P. Schlottmann, *Journal of Physics: Condensed Matter* **1**, 10193 (1989).
 - [27] S. Xu, J. T. Barreiro, Y. Wang, and C. Wu, *Physical Review Letters* **121**, 167205 (2018).
 - [28] S. Moulder, S. Beattie, R. P. Smith, N. Tammuz, and Z. Hadzibabic, *Physical Review A* **86**, 013629 (2012).
 - [29] K. C. Wright, R. B. Blakestad, C. J. Lobb, W. D. Phillips, and G. K. Campbell, *Phys. Rev. Lett.* **110**, 025302 (2013).
 - [30] M. N. Barber, *Phase transitions and critical phenomena* **8** (1983).
 - [31] P. Schlottmann, *Physical Review B* **45**, 5784 (1992).
 - [32] S. R. Manmana, K. R. Hazzard, G. Chen, A. E. Feiguin, and A. M. Rey, *Physical Review A* **84**, 043601 (2011).
 - [33] R. Assaraf, P. Azaria, M. Caffarel, and P. Lecheminant, *Physical Review B* **60**, 2299 (1999).
 - [34] K. Bucht, Ö. Legeza, E. Szirmai, and J. Sólyom, *Physical Review B* **75**, 155108 (2007).
 - [35] X. Waintal, G. Fleury, K. Kazymyrenko, M. Houzet, P. Schmitteckert, and D. Weinmann, *Physical review letters* **101**, 106804 (2008).
 - [36] B. J. DeSalvo, M. Yan, P. G. Mickelson, Y. N. Martinez de Escobar, and T. C. Killian, *Phys. Rev. Lett.* **105**, 030402 (2010).
 - [37] S. Stellmer, R. Grimm, and F. Schreck, *Phys. Rev. A* **87**, 013611 (2013).
 - [38] F. Bloch, *Phys. Rev. A* **7**, 2187 (1973).

Supplementary material

Persistent Current of $SU(N)$ Fermions.

In the following sections, we provide supporting details of the theory discussed in the main manuscript.

The derivation of the persistent current for $SU(N)$ fermions is sketched out in the limit of infinite interaction U . The analytics are carried out for the two integrable limits of the Hubbard model: incommensurate low filling fractions and integer fillings. A specific analysis is devoted to the energy and consequently the persistent current at large but finite U . The persistent current undergoes a non-trivial change of the bare flux quantum. This feature occurs because of the presence of spinons in the ground state of the system. Spinons of different types correspond to specific Bethe quantum numbers configurations. The Bethe quantum number configurations needed for the given value of X are provided. We then proceed to discuss $|\phi_s - \phi_d|$ providing the figure of merit for the generation of spinons. Spinon generation is inhibited for commensurate fillings due to a spectral gap that opens up for a finite value of U . Lastly, the parity effect for incommensurate systems is considered.

Derivation of the Persistent Current in the limit of infinite U for $SU(N)$ Fermions

The derivation of the persistent current for $SU(N)$ fermions in the limit of infinite interaction U , is sketched out for the two integrable limits of the $SU(N)$ Hubbard model.

A system of interacting fermions with $SU(N)$ spin symmetry residing on a chain of length L threaded by an effective magnetic flux ϕ , is described by the Gaudin-Yang-Sutherland model [14, 23],

$$\mathcal{H} = - \sum_{m=1}^N \sum_{i=1}^{N_m} \left(-i \frac{\partial}{\partial x_{i,m}} - \frac{2\pi}{L} \phi \right)^2 + 4U \sum_{i < j, m, n} \delta(x_{i,m} - x_{j,n}) \quad (1)$$

where N_p is the number of electrons with colour α of $SU(N)$ symmetry with $m = 1, \dots, N$. The model is integrable by Bethe ansatz and is given by the following set of equations.

$$e^{i(k_j L - \phi)} = \prod_{\alpha=1}^{M_1} \frac{4(k_j - \lambda_{\alpha}^{(1)}) + iU}{4(k_j - \lambda_{\alpha}^{(1)}) - iU} \quad j = 1, \dots, N_p \quad (2)$$

$$\prod_{\beta \neq \alpha}^{M_r} \frac{2(\lambda_{\alpha}^{(r)} - \lambda_{\beta}^{(r)}) + iU}{2(\lambda_{\alpha}^{(r)} - \lambda_{\beta}^{(r)}) - iU} = \prod_{\beta=1}^{M_{r-1}} \frac{4(\lambda_{\alpha}^{(r)} - \lambda_{\beta}^{(r-1)}) + iU}{4(\lambda_{\alpha}^{(r)} - \lambda_{\beta}^{(r-1)}) - iU} \cdot \prod_{\beta=1}^{M_{r+1}} \frac{4(\lambda_{\alpha}^{(r)} - \lambda_{\beta}^{(r+1)}) + iU}{4(\lambda_{\alpha}^{(r)} - \lambda_{\beta}^{(r+1)}) - iU} \quad \alpha = 1, \dots, M_r \quad (3)$$

for $r = 1, \dots, N-1$ where $M_0 = N_p$, $M_N = 0$ and $\lambda_{\beta}^{(0)} = k_{\beta}$. N_p denotes the number of particles, M_r corresponds to the colour with k_j and $\lambda_{\alpha}^{(r)}$ being the charge and spin momenta respectively. The energy corresponding to the state for every solution of these equations is $E = \sum_j^{N_p} k_j^2$.

Taking the $SU(3)$ case as an example, one obtains a set consisting of three non-linear equations

$$e^{ik_j L} = \prod_{\alpha=1}^{M_1} \frac{4(k_j - \lambda_{\alpha}^{(1)}) + iU}{4(k_j - \lambda_{\alpha}^{(1)}) - iU} \quad (4)$$

$$\prod_{\beta \neq \alpha}^{M_1} \frac{2(\lambda_{\alpha}^{(1)} - \lambda_{\beta}^{(1)}) + iU}{2(\lambda_{\alpha}^{(1)} - \lambda_{\beta}^{(1)}) - iU} = \prod_{\beta=1}^{M_0=N_p} \frac{4(\lambda_{\alpha}^{(1)} - k_{\beta}) + iU}{4(\lambda_{\alpha}^{(1)} - k_{\beta}) - iU} \prod_{\beta=1}^{M_2} \frac{4(\lambda_{\alpha}^{(1)} - \lambda_{\beta}^{(2)}) + iU}{4(\lambda_{\alpha}^{(1)} - \lambda_{\beta}^{(2)}) - iU} \quad (5)$$

$$\prod_{\beta \neq \alpha}^{M_2} \frac{2(\lambda_{\alpha}^{(2)} - \lambda_{\beta}^{(2)}) + iU}{2(\lambda_{\alpha}^{(2)} - \lambda_{\beta}^{(2)}) - iU} = \prod_{\beta=1}^{M_1} \frac{4(\lambda_{\alpha}^{(2)} - \lambda_{\beta}^{(1)}) + iU}{4(\lambda_{\alpha}^{(2)} - \lambda_{\beta}^{(1)}) - iU} \quad (6)$$

which can be re-written in logarithmic form as

$$k_j L + 2 \sum_{\alpha=1}^{M_1} \arctan\left(\frac{4(k_j - \lambda_{\alpha}^{(1)})}{U}\right) = 2\pi(I_j + \phi) \quad j = 1, \dots, N_p \quad (7)$$

$$2 \sum_{\beta=1}^{N_p} \arctan\left(\frac{4(\lambda_{\alpha}^{(1)} - k_{\beta})}{U}\right) + 2 \sum_{a=1}^{M_2} \arctan\left(\frac{4(\lambda_{\alpha}^{(1)} - l_a)}{U}\right) - 2 \sum_{\beta=1}^{M_1} \arctan\left(\frac{2(\lambda_{\alpha}^{(1)} - \lambda_{\beta}^{(1)})}{U}\right) = 2\pi J_{\alpha} \quad \alpha = 1, \dots, M_1 \quad (8)$$

$$2 \sum_{\beta=1}^{M_1} \arctan\left(\frac{4(l_a - \lambda_{\beta}^{(1)})}{U}\right) - 2 \sum_{b=1}^{M_2} \arctan\left(\frac{2(l_a - l_b)}{U}\right) = 2\pi L_a \quad a = 1, \dots, M_2 \quad (9)$$

where $\lambda_{\beta}^{(2)}$ was changed to l_a for the sake of convenience with I_j , J_{α} and L_a being the Bethe quantum numbers, the first being associated with charge momenta and the other two for spin momenta. Carrying out a summation over α and over a for Equations (8) and (9) respectively,

$$2 \sum_{\alpha=1}^{M_1} \sum_{\beta=1}^{N_p} \arctan\left(\frac{4(\lambda_{\alpha}^{(1)} - k_{\beta})}{U}\right) + 2 \sum_{\alpha=1}^{M_1} \sum_{a=1}^{M_2} \arctan\left(\frac{4(\lambda_{\alpha}^{(1)} - l_a)}{U}\right) - 2 \sum_{\alpha=1}^{M_1} \sum_{\beta=1}^{M_1} \arctan\left(\frac{2(\lambda_{\alpha}^{(1)} - \lambda_{\beta}^{(1)})}{U}\right) = 2\pi \sum_{\alpha=1}^{M_1} J_{\alpha} \quad (10)$$

$$2 \sum_{a=1}^{M_2} \sum_{\beta=1}^{M_1} \arctan\left(\frac{4(l_a - \lambda_{\beta}^{(1)})}{U}\right) - 2 \sum_{a=1}^{M_2} \sum_{b=1}^{M_2} \arctan\left(\frac{2(l_a - l_b)}{U}\right) = 2\pi \sum_{a=1}^{M_2} L_a \quad a = 1, \dots, M_2 \quad (11)$$

and noting that the last term on the left hand side in both of the above equations goes to zero, leads one to the following expression

$$2 \sum_{\alpha=1}^{M_1} \sum_{\beta=1}^{N_p} \arctan\left(\frac{4(\lambda_{\alpha}^{(1)} - k_{\beta})}{U}\right) = 2\pi \left(\sum_{\alpha=1}^{M_1} J_{\alpha} + \sum_{a=1}^{M_2} L_a \right) \quad (12)$$

In the limit $\frac{U}{N_p} \rightarrow \infty$, the k_j terms can be neglected since they are significantly smaller in magnitude compared to the spin momenta. Consequently,

$$2 \sum_{\alpha=1}^{M_1} \sum_{\beta=1}^{N_p} \arctan\left(\frac{4\lambda_{\alpha}^{(1)}}{U}\right) = 2\pi \left(\sum_{\alpha=1}^{M_1} J_{\alpha} + \sum_{a=1}^{M_2} L_a \right) \Rightarrow 2 \sum_{\alpha=1}^{M_1} \arctan\left(\frac{4\lambda_{\alpha}^{(1)}}{U}\right) = \frac{2\pi}{N_p} \left(\sum_{\alpha=1}^{M_1} J_{\alpha} + \sum_{a=1}^{M_2} L_a \right) \quad (13)$$

which upon substitution in Equation (7) yields

$$k_j L = 2\pi \left[I_j + \frac{1}{N_p} \left(\sum_{\alpha=1}^{M_1} J_{\alpha} + \sum_{a=1}^{M_2} L_a \right) + \phi \right] \quad (14)$$

Squaring the above expression,

$$k_j^2 = \left(\frac{2\pi}{L} \right)^2 \left[I_j^2 + 2I_j \left(\frac{X}{N_p} + \phi \right) + \left(\frac{X}{N_p} \right)^2 + 2\phi \frac{X}{N_p} + \phi^2 \right] \quad (15)$$

the ground state energy of the system is given by

$$E_0 = \sum_j^{N_p} k_j^2 = \left(\frac{2\pi}{L} \right)^2 \left[\sum_j^{N_p} I_j^2 + 2 \sum_j^{N_p} I_j \left(\frac{X}{N_p} + \phi \right) + \left(\frac{X}{N_p} \right)^2 + N_p \left(2\phi \frac{X}{N_p} + \phi^2 \right) \right] \quad (16)$$

assuming the I_j quantum numbers are a consecutive integer/half-integer set, where $X = \left(\sum_{\alpha=1}^{M_1} J_{\alpha} + \sum_{a=1}^{M_2} L_a \right)$. At zero temperature the persistent current of the system is defined as,

$$I(\phi) = -\frac{\partial E_0}{\partial \phi} \quad (17)$$

Therefore, the persistent current in the limit of infinite U turns out to be,

$$I(\phi) = -2 \left(\frac{2\pi}{L} \right)^2 \sum_j^{N_p} \left[I_j + \frac{X}{N_p} + \phi \right] \quad (18)$$

In the case of $SU(N)$ fermions, one would still have the same expression for the persistent current. The only difference is that $X = \sum_j^{N-1} \sum_{\alpha_j} J_{\alpha_j}$.

The other integrable limit of the $SU(N)$ Hubbard model, is for commensurate filling fractions in the presence of a lattice.

The model is described by the Lai-Sutherland model [10, 18] with the energy of the system being given by $E = -2 \sum_j^{N_p} \cos k_j$.

The Bethe ansatz equations for this model are similar to the ones outlined in Equations (2) and (3). However, in this case in Equation (2) there is $\sin k_j$ instead of k_j on the right hand side and for Equation (3) one substitutes $\lambda_{\beta}^{(0)} = \sin k_{\beta}$ when required. By following the same procedure one arrives to Equation (14). Substituting this expression in the energy of the system, one arrives to

$$E_0(\phi) = -E_m \cos \left[\frac{2\pi}{L} \left(D + \frac{X}{N_p} + \phi \right) \right] \quad (19)$$

and in turn the persistent current is of the following form,

$$I(\phi) = -E_m \left(\frac{2\pi}{L} \right) \sin \left[\frac{2\pi}{L} \left(D + \frac{X}{N_p} + \phi \right) \right] \quad (20)$$

where $E_m = 2 \frac{\sin(\frac{N_p \pi}{L})}{\sin(\frac{\pi}{L})}$ where $D = \frac{I_{max} + I_{min}}{2}$, which comes about due to the I_j being consecutive for the ground state configuration.

The above expression is a generalization of the ground state energy for $SU(2)$ fermions obtained in [15, 16]. In particular, at infinite U for the same number of particles the pre-factor E_m is the same for $SU(N)$ as it was for $SU(2)$. This in turn implies that the ground state energy for fermions carrying different $SU(N)$ spin, say $SU(2)$ and $SU(3)$, will coincide if their phase shift is the same. The same also holds true for expression (16).

Corrections to the infinite U limit: derivation of the Energy Spin correction

In this section we generalize the energy spin correction, obtained for $SU(2)$ fermions in [16], for $SU(N)$ fermions. At infinite U the system is highly degenerate, meaning that there are multiple ways of choosing the spin rapidity J_{α} distribution [15, 16]. In order to find out the lowest energy state at finite U when the degeneracy is lifted, leading order $\frac{1}{U}$ corrections have to be introduced for the Bethe ansatz equations at infinite U . When U is at infinity, the charge momenta k_j are of order unity whilst the spin momenta λ_{β} are of order U . With this picture in mind, we expand the arctangent function in Equation (7) to leading order in $\frac{k_j}{U}$. Defining the scaled variables x_{α} as,

$$x_{\alpha} = \lim_{U \rightarrow \infty} \left(\frac{2\lambda_{\alpha}}{U} \right) \quad (21)$$

through Taylor expansion one finds that,

$$f(x+h) = \arctan(2x_{\alpha}) - 2 \frac{k_j}{U} \frac{1}{x_{\alpha}^2 + \frac{1}{4}} \quad (22)$$

Therefore, for large but finite U , the k_j have leading $\frac{1}{U}$ corrections,

$$\delta k_j = -2 \frac{k_j}{UL} \sum_{\alpha}^M \frac{1}{x_{\alpha}^2 + \frac{1}{4}} \quad (23)$$

where the x_{α} has to satisfy the remaining Bethe equations which in the $SU(3)$ case for example are Equations (9) and (10). The total ground state energy reads,

$$E = \sum_j^{N_p} (k_j + \delta k_j)^2 = \sum_{j=1}^{N_p} \left(k_j^2 + 2k_j \delta k_j + (\delta k_j)^2 \right) \quad (24)$$

Therefore, the leading order $\frac{1}{U}$ correction is given by

$$+ 2k_j \delta k_j = -\frac{4}{UL} \sum_j^{N_p} k_j^2 \sum_\alpha^M \frac{1}{x_\alpha^2 + \frac{1}{4}} = J_{eff} \sum_\alpha^M \frac{1}{x_\alpha^2 + \frac{1}{4}} \quad (25)$$

In the presence of a lattice, the energy correction is of a similar form

$$+ 2\delta k_j \sin(k_j) = J_{eff} \sum_\alpha^M \frac{1}{x_\alpha^2 + \frac{1}{4}} \quad (26)$$

but $J_{eff} = -\frac{4}{UL} \left(\sum_{j=1}^{N_p} \sin^2 k_j \right)$ in this case, whereby k_j in Equation (25) was replaced by $\sin k_j$. The leading order $\frac{1}{U}$ correction to the Bethe ansatz equations for $SU(N)$ fermions has the same expression as the one obtained for $SU(2)$ in [16]. This was to be expected since Equation (7), which is the primary equation relating the charge and spin rapidities, is the same for all $SU(N)$.

Bethe Ansatz Spinon Configurations

To obtain the minimum energy for a given value of the flux ϕ , one requires that the summation over the spin rapidities satisfies the degeneracy point equation having the form [15, 16]

$$\frac{2w-1}{2N_p} \leq \phi + D \leq \frac{2w+1}{2N_p} \quad \text{where} \quad X = -w \quad (27)$$

with w only being allowed to have integer or half-integer values due to the nature of the spin rapidities.

Consider the case of three fermions with $SU(3)$ spin. There are three sets of quantum numbers: one pertaining to the charge momenta I_j and the other two belonging to the spin momenta denoted as J_{α_1} and J_{α_2} . The ground state configuration for such a system is given as $I_j = \{-1, 0, 1\}$, $J_{\alpha_1} = \{-0.5, 0.5\}$ and $J_{\alpha_2} = \{0\}$. The correction of the spin quantum numbers for all the values of the flux per Equation (25) is as follows

Magnetic flux	J_{α_1}	J_{α_2}	X
0.0 – 0.1	$\{-0.5, 0.5\}$	$\{0\}$	0
0.2 – 0.5	$\{-1.5, 0.5\}$	$\{0\}$	-1
0.6 – 0.8	$\{-0.5, 1.5\}$	$\{0\}$	+1
0.9 – 1.0	$\{-0.5, 0.5\}$	$\{0\}$	0

TABLE I. Spin quantum number configurations with the flux for $N_p = 3$ with $SU(3)$ spin with $M_1 = 2$ and $M_2 = 1$.

As can be seen from Table (I), in cases where $X = 0$, the spin quantum number configuration is different from the ground state one and ‘holes’ are introduced such that the spin quantum number configurations are no longer consecutive, with the I_j set remaining unchanged. There are two notable points worthy of mention. The first is that one could have chosen a different way to arrange the set of quantum numbers. An alternative arrangement is given by Table (II). The target value X is reached via a different configuration, which in turn leads to a degenerate state. Such a phenomenon is a characteristic property of $SU(N)$ systems that is not present for $SU(2)$. As N increases, the number of degenerate states that are present in the system increases due to the various Bethe quantum number configurations that one can adopt.

Magnetic flux	J_{α_1}	J_{α_2}	X
0.0 – 0.1	$\{-0.5, 0.5\}$	$\{0\}$	0
0.2 – 0.5	$\{-0.5, 0.5\}$	$\{-1\}$	-1
0.6 – 0.8	$\{-0.5, 0.5\}$	$\{+1\}$	+1
0.9 – 1.0	$\{-0.5, 0.5\}$	$\{0\}$	0

TABLE II. Alternative spin quantum number configurations with the flux for $N_p = 3$ with $SU(3)$ spin with $M_1 = 2$ and $M_2 = 1$.

The other point concerns the value of X for $\phi = 0.6 - 0.8$ and $\phi = 0.9 - 1.0$. According to Equation (27), X should be equal to -2 and -3 respectively. The reason behind this is due to the fact that the degeneracy equation has to be applied within a specific

flux range that depends on the parity of the system: for a flux in the interval of -0.5 to 0.5 for $N_p = N(2n+1)$ and in the range of $\phi = 0.0$ to 1.0 in the case of $N_p = N(2n)$. The ground state energy of the system is given by a series of parabolas in the absence of an effective magnetic flux. These parabolas each have a well defined angular momentum l . They intersect at the degeneracy points, which is parity dependent, and are shifted with respect to each other by a Galilean translation [38]. Consequently, when the magnetic flux piercing the system falls outside the range outlined previously, one needs to change the I_j quantum numbers in order to offset the increase in angular momentum l that one obtains on going to the next energy parabola.

For positive ϕ one requires that the I_j quantum numbers need to all be shifted by one to the left. For example in the case considered above for $\phi > 0.5$, the I_j go from $\{-1, 0, 1\}$ to $\{-2, -1, 0\}$ for $0.5 < \phi < 1.5$. On going to the next parabola, they would need to be shifted again by one to the left. In the case of negative ϕ , the shift occurs to the right.

Note that there are other combinations of the quantum numbers, not outlined in Tables I and II, whose total sum reaches the target value of X . However, these configurations do not give the lowest value for the energy as the ones mentioned, even though the value of X is the same. At infinite U , the system is solely dependent on the value of X and not on the arrangement of the spin quantum number configuration. Consequently, the system is highly degenerate. This is also observed in the $SU(2)$ case. However, as mentioned in the derivation of the energy correction, the degeneracy is lifted on going to large but finite U and one is left with only one combination that gives the lowest energy in the case of $SU(2)$ systems. On the other hand, for $SU(N)$ systems whilst this degeneracy is also lifted, they also benefit from an extra ‘source’ of degeneracy due to the different configurations of the Bethe quantum numbers as shown in Tables I and II.

Spinon creation in the groundstate $SU(N)$ Fermions

The $SU(N)$ Hubbard model is not integrable in all limits, unlike its $SU(2)$ counterpart. The Hamiltonian is integrable by Bethe ansatz for incommensurate and commensurate filling fractions. In this section, we take a look at spinon creation for $SU(N)$ fermions in these two regimes.

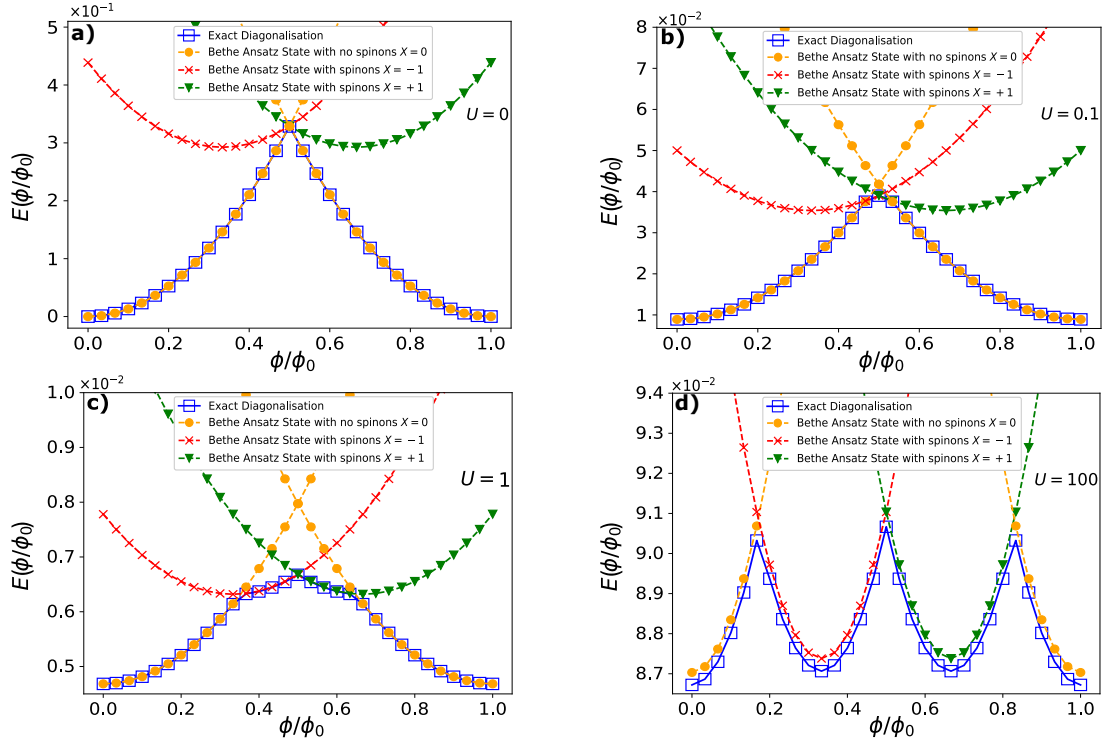


FIG. 6. Spinon creation in incommensurate $SU(N)$ fermionic systems. The case of $N = 3$ is considered for $N_p = 3$ fermions residing on a ring composed of $L = 30$ sites. The above figures show how the Bethe ansatz energies need to be characterized by spinon quantum numbers in order to have the actual ground state for various values of the interaction U . All curves are calculated with the Bethe ansatz of the Gaudin-Yang-Sutherland model and exact diagonalization.

For a system with incommensurate filling fractions, spinons are created with increasing U as can be observed from Fig. 6. Level crossings occur between the groundstate with no spinons and levels with spinon character X , with the value of X obtained as outlined in the previous section. The creation of spinons starts out around the degeneracy point ϕ_d (see Fig. 6b), which is parity dependent. The degeneracy point ϕ_d is 0 for $N_p = N(2n)$ and 0.5 for $N_p = N(2n + 1)$ systems. Comparing Fig. 6a and Fig. 6d, we observe that the elementary flux quantum ϕ_0 has been renormalized in the latter case and that $1/N_p$ periodicity is achieved, resulting in N_p cusps/parabolic-wise segments that corresponds to 3 in this case.

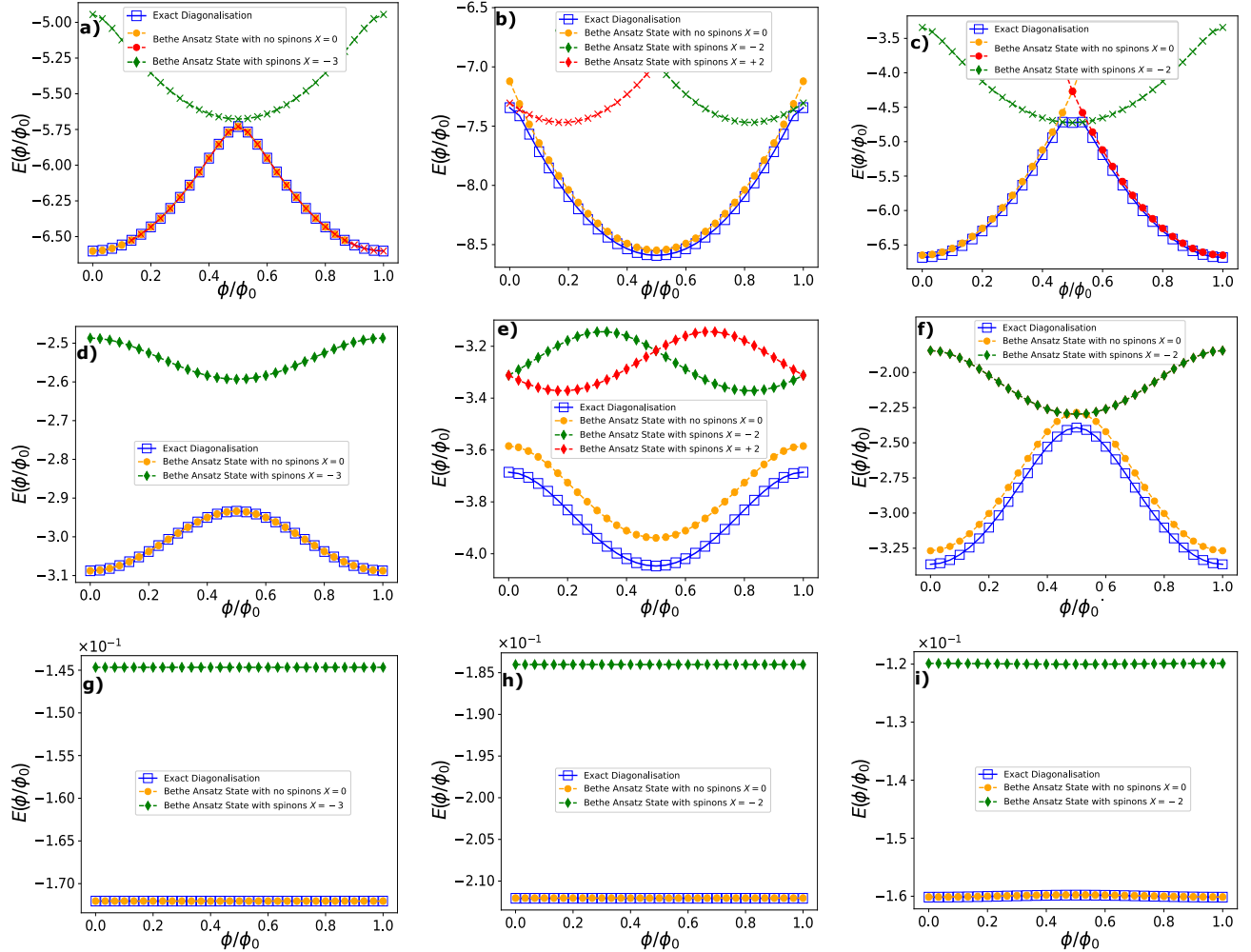


FIG. 7. Spinon creation in commensurate $SU(N)$ fermionic systems. The systems taken in consideration are $SU(2)$ with $N_p = 6$ (left column), $SU(3)$ with $N_p = 6$ (middle column) and $SU(4)$ with $N_p = 4$ (right column). The different Bethe ansatz energies of the Lai-Sutherland model characterized by different spinon configurations needed to make up the ground state of the system are considered for different values of interaction with $U = 1$ (top row), $U = 5$ (middle row) and $U = 100$ (last row). All the presented results are obtained with Bethe ansatz of the Gaudin-Yang-Sutherland model for $N_p = L$. The Bethe ansatz states with no spinons, having two different colours (orange and red), are used to indicate that the I_j quantum numbers are shifted due to being in different energy parabolas. In the case of $U = 1$, the Bethe ansatz did not converge for certain values of the flux. This does not have an impact on what we are trying to discuss here and so they were left out.

In the case of commensurate filling fractions, spinon creation is drastically impacted by a spectral gap that opens around the transition to the Mott phase (see Fig. 8). The energy gap is determined as the minimal gap for any flux $\Delta E = \min_\phi(\Delta E)$. For the special case $N = 2$, the gap opens at $U = 0$, whereas for any other N it opens at non-zero U indicating the onset to the Mott phase transition. Indeed if spinon creation in a system with $SU(2)$ fermions (Figs. 7a,d,g)) is compared to systems with $SU(3)$ (Figs. 7b,e,h)) and $SU(4)$ (Figs. 7c,f,i)) spin components, we note that no spinons are created in the $SU(2)$ case for any value of U . On the other hand for $SU(N)$ systems, spinon creation is present in the system for values of U below the threshold value of where the transition happens U^* , which was calculated to be around 2.9. An interesting feature that pops up, is that after passing U^* , one no longer needs to change the I_j quantum numbers on going from one energy parabola to the other, as can be seen by comparing (Figs. 7c,f)).

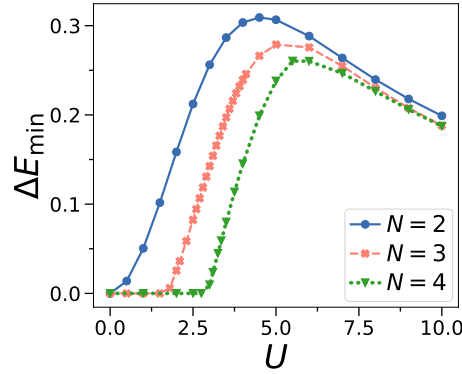


FIG. 8. $SU(N)$ energy gap at integer filling. Minimal energy gap $E_{\min} = \min_{\phi}(\Delta E)$ for different N against U at comparable system sizes ($N = 2$ and $N = 4$ with $L = 8$ and $N = 3$ with $L = 9$). All curves were obtained by exact diagonalization.

Due to the specific $N-1$ types of excitations that are inherently present in $SU(N)$ fermions for $N > 2$, spinon creation is facilitated with N . This can be clearly seen from Figs. 9a),b). In the case where $N_p/N > 1$, discontinuities arise in the intermediate U regime as can be seen from the insets of Figs. 9a),b). The discontinuities arise due to jumps ΔX in the spinon character X and are absent when $N_p/N = 1$ (inset of Fig. 9a). Additionally, when comparing systems containing the same N_p , the discontinuities tend to smoothen out with increasing N and L . This can be clearly seen from Figs. 9b),c)

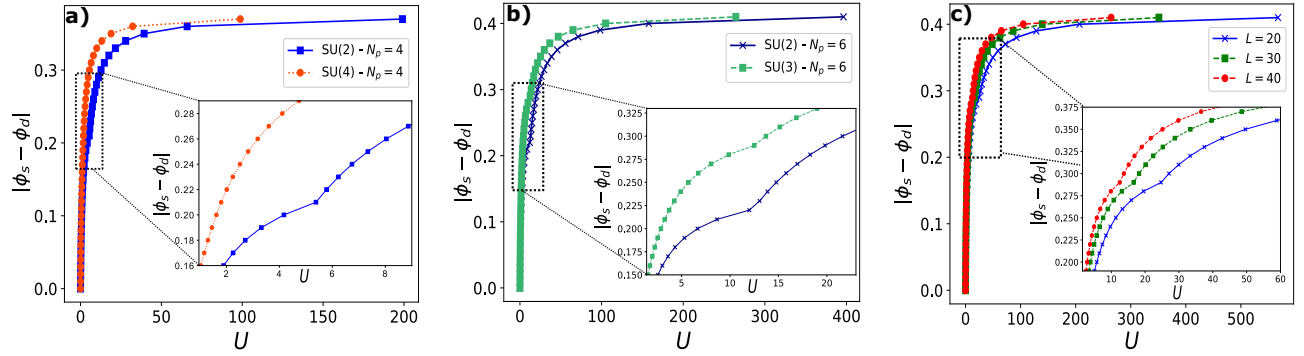


FIG. 9. Comparison of spinon creation in $SU(2)$ fermions and $SU(N)$ fermions. a) Spinon creation flux distance $|\phi_s - \phi_d|$ against interaction U is considered for a ring of $L = 40$ sites with $N_p = 4$ fermions with $N = 2$ and $N = 4$ spin components, where ϕ_s is the flux at which spinons are created and ϕ_d is the degeneracy point. The intermediate U regime (inset) highlights the discontinuity present in the $SU(2)$ case. b) Spinon creation flux distance against interaction for a ring of $L = 40$ sites with $N_p = 6$ fermions with $N = 2$ and $N = 3$ spin components. The inset depicts the discontinuities for intermediate U in both systems. c) Spinon creation is for a system with $N_p = 6$ particles with $N = 3$ with various system sizes, $L = 20$, $L = 30$ and $L = 40$. All the presented results are obtained with Bethe ansatz of the Gaudin-Yang-Sutherland model.

Parity effect

A specific parity effect is observed in $SU(N)$ systems. When the number of particles in the systems is given by $N_p = N(2n + 1)$, the persistent current is diamagnetic. On the other hand, the persistent current is paramagnetic for $N_p = N(2n)$ where n is an integer starting from 0. The diamagnetic (paramagnetic) nature of the current is characterized by having a minimum (maximum) of the ground state energy at zero flux. On going to infinite U , the parity effect is washed out. This occurs due to the change in periodicity of the elementary flux. The renormalization of the flux causes the ground state energy to be minimum at zero flux. Consequently, the persistent current becomes diamagnetic. In the cases where the current already had a diamagnetic nature at small values of U , its nature remains unchanged. The washing out of the persistent current can be clearly observed from Fig. 10 whereby comparison of $SU(3)$ systems with $N_p = 3$ and $N_p = 6$ clearly show the stark difference in the nature of the current for the latter case between the different regimes of U .

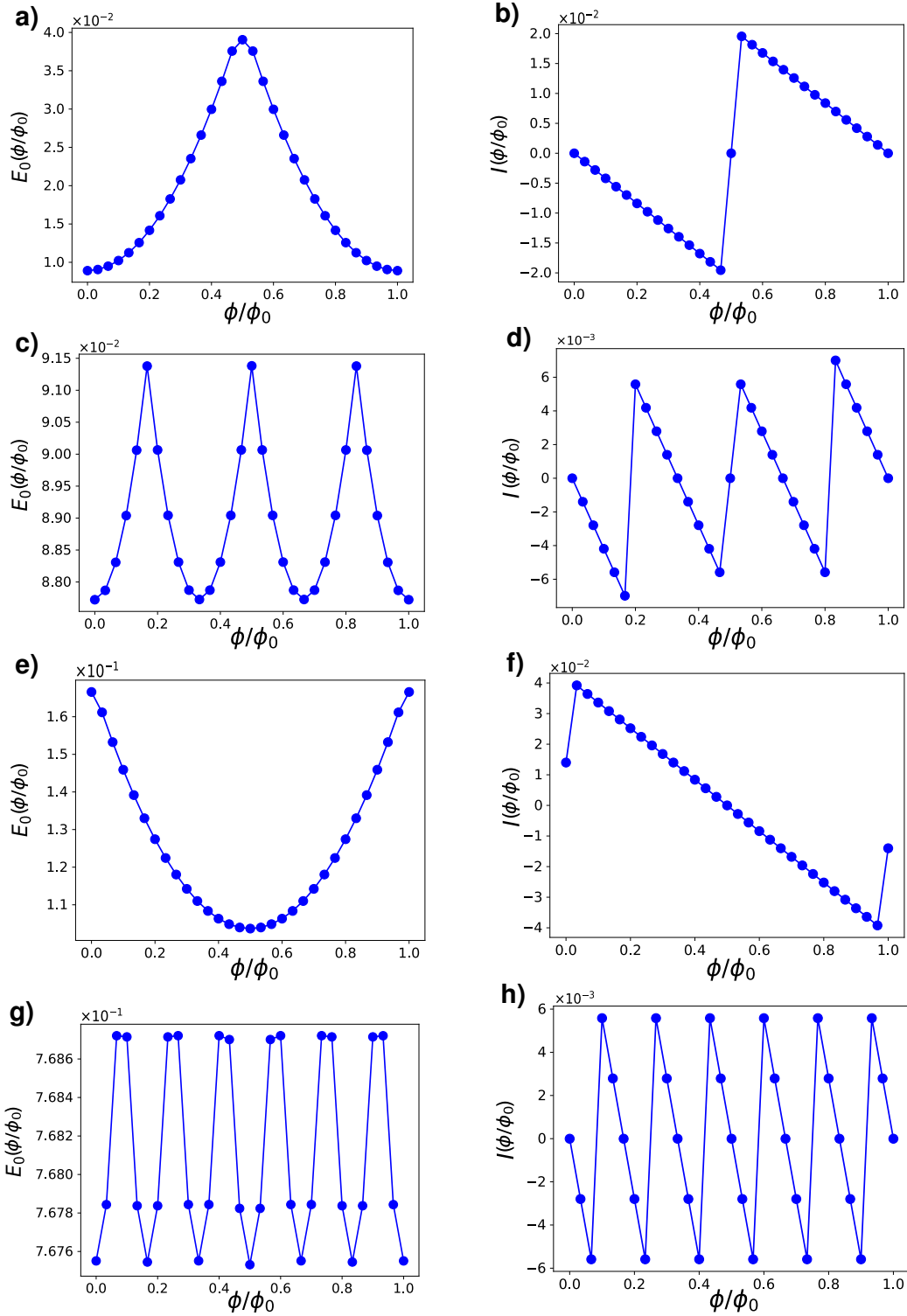


FIG. 10. $SU(N)$ persistent current and the corresponding ground state energy at incommensurate filling for different interaction strengths U . **a),b)** Ground state energy and Persistent current for $N_p = 3$ for $U = 0.1$. **c),d)** Ground state energy and Persistent current for $N_p = 3$ for $U = 10,000$. **e),f)** Ground state energy and Persistent current for $N_p = 6$ for $U = 0.1$. **g),h)** Ground state energy and Persistent current for $N_p = 6$ for $U = 10,000$. All curves are calculated with Bethe ansatz for the Gaudin-Yang-Sutherland model with $L = 30$.